http://dx.doi.org/10.5012/bkcs.2011.32.9.3372

Determination of Atomic Structures and Relative Stabilities of Diadduct Regioisomers of $C_{20}X_2$ (X = H, F, Cl, Br, and OH) by the Hybrid Density-Functional B3LYP Method

Seol Lee, Youngsun Suh, Yong Gyoo Hwang,[†,*] and Kee Hag Lee[*]

Department of Chemistry, and Nanoscale Sciences and Technology Institute, Wonkwang University, Iksan, Jeonbuk 570-749, Korea. [*]E-mail: khlee@wonkwang.ac.kr
[†]Division of Microelectronics and Display Technology, and Nanoscale Sciences and Technology Institute, Wonkwang University, Iksan, Jeonbuk 570-749, Korea. [*]E-mail: yghwang@wonkwang.ac.kr
Received June 9, 2011, Accepted July 27, 2011

We have studied the relative stability and atomic structures of five $C_{20}X_2$ regioisomers obtained as diadducts of a C_{20} cage (X = H, F, Cl, Br, and OH). All the regioisomers are geometric isomers, i.e., they differ in their spatial arrangement. Full-geometry optimizations of the regioisomers have been performed using the hybrid density-functional (B3LYP/6-31G(d, p)) method. Our results suggest that the *cis*-1 regioisomer (the 1,2-diadduct) is the most stable and that the second most stable is the *trans*-2 (1,13-diadduct) regioisomer, implying that the long-range interaction between the two adducts and the resonance effect are more pronounced than the diadduct-induced strain in the C_{20} cage. The HOMO and LUMO characteristics of each regioisomer with the same symmetry of structural regioisomers except $C_{20}(OH)_2$ are topologically same. This suggests that by using an entirely different set of characteristic chemical reactions for each regioisomer, we can distinguish between the five regioisomers for each C_{20} diadduct derivative.

Key Words : C_{20} diadducts (dihydride, dihydroxide, and dihalides), $C_{20}X_2$ regioisomers, Hybrid density-functional (B3LYP) calculations, HOMO and LUMO

Introduction

The geometry of fullerenes obeys the isolated-pentagon rule (IPR), which states that the most stable fullerenes are those in which all pentagons (5-membered rings, 5-MRs) located as far as possible from one another and are surrounded by five hexagons (6-membered rings, 6-MRs).[1,2] However, it is impossible to satisfy this rule for the smallest possible fullerene, C_{20} (first synthesized in 2000), which contains only 12 5-MRs and no 6-MRs.[3] This implies that this non-IPR fullerene should be highly reactive owing to the fusion of the strained 5-MRs. Because C_{20} can relieve this strain through sp^3-bond-forming reactions, the formation of isomeric derivatives is expected. As the C_{20} cage would be one of the candidates of molecular devices, modification of the structural and electronic properties of C_{20} should be a subject of general interest to both experimentalists and theoreticians.

Isomerism in chemistry is a fundamental concept, and the term "regioisomer" refers to a type of structural isomer. In the formation of regioisomers, regioselectivity is observed in the chemical reactions of molecules for which there are choices of different orientations or reaction sites. As opposed to fullerene C_{20} derivatives that have only 5-MRs, the regioisomers of various kinds of derivatives, including diadducts of fullerene with 5- and 6-MRs, have been extensively studied.[4,5] The gas-phase production of $C_{20}Br_2$ and $C_{20}H_2$ has been reported.[6,7] Experimental examples that show the relative stability of C_{20} regioisomers are very few in number. Proton transfer between the -OH groups of two $C_{20}(OH_2)_2$ molecules was examined by *ab initio* molecular orbital calculations.[8] The adducts of the most stable one among the parent fullerene C_{20} isomers with C_2H_2 and C_2H_4 have been studied by the B3LYP method: the derivatives $C_{20}(C_2H_2)_n$ and $C_{20}(C_2H_4)_n$ (n = 1-3) exhibit remarkable aromaticity, while $C_{20}(C_2H_2)_4$ and $C_{20}(C_2H_4)_4$ have no spherical aromaticity.[9] Moreover, the highest occupied molecular orbital (HOMO) and the lowest unoccupied molecular orbital (LUMO) maps suggest that the five bond-stretched isomers of the C_{20} dication can be verified by chemical addition reactions.[10]

To the best of our knowledge, the evaluation of fullerene $C_{20}X_2$ diadduct regioisomers by the first-principle hybrid density-functional B3LYP method has received scant attention. In this study, we would like to report the relative stability and electronic structures of fullerene diadduct $C_{20}X_2$ regioisomers, where X is H, F, Cl, Br, or OH.

Recently, the planarity of benzene was analyzed using various theoretical methods, and the B3LYP/6-31G(d) level calculation was found to be suitable for simulating the experimentally determined structure of benzene.[11]

To the best of our knowledge, no calculations have been performed for the full optimization of $C_{20}X_2$ (X = H, F, Cl, Br, and OH) regioisomers at the level of B3LYP/6-31G(d, p), even though many calculations have been reported for the parent C_{20} cage[9] as well as $C_{20}H_{20}$ dodecahedrane[12] and

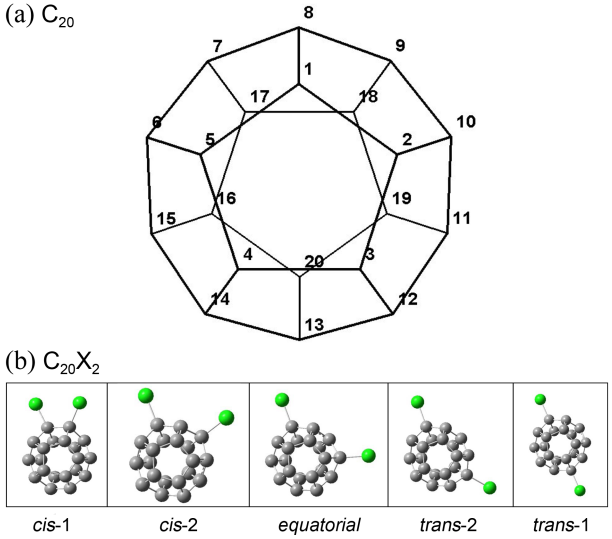

Figure 1. C_{20} cluster cage with carbon numbering used to distinguish between the different regioisomeric derivatives. Here, X = H, F, Cl, Br, or OH.

$C_{20}F_{20}$ perfluorododecahedrane.[13,14] In this study, we obtained the relative energies and atomic structures for the $C_{20}X_2$ regioisomers having the same spin state. Although the predominant electronic configurations of the regioisomers would be similar, the HOMO and LUMO maps would be different for the different derivatives. If so, we can anticipate an entirely different set of characteristic chemical reactions for the exohedral complexes, on the basis of the HOMO and LUMO for each type of derivative.

Calculations

In this study, the hybrid density-functional theory (DFT) with Becke's three-parameter hybrid method and the Lee-Yang-Parr exchange-correlation functional theory (B3LYP)[15-17] were used to optimize the geometries of the $C_{20}X_2$ (X = H, F, Cl, Br, and OH) regioisomers. The electron basis set 6-31G(d, p) was used throughout this study.[18] We fully optimized all the geometries of the $C_{20}X_2$ derivative regioisomers using the Gaussian 03 B.04 package suite.[19] To

Table 2. The HOMO and LUMO energies (eV), the enegy gap (Δε) between the HOMO and LUMO energies, strain energies (kJ/mol), and the distance between the two adducts of $C_{20}X_2$ (X = H, F, Cl, Br, and OH) regioisomers at the level of B3LYP/6-31G(d, p) calculations

$C_{20}H_2$	Distance (Å)	HOMO (eV)	LUMO (eV)	Δε (eV)	Strain E (kJ/mol)
cis-1	2.537	-5.388	-2.748	2.640	109.7
cis-2	3.915	-5.687	-2.803	2.884	97.4
equatorial	5.472	-5.225	-2.803	2.422	110.0
trans-2	6.310	-5.606	-2.694	2.912	131.3
trans-1	6.655	-4.653	-2.503	2.150	153.1
$C_{20}F_2$					
cis-1	2.696	-6.068	-3.293	2.776	103.7
cis-2	4.205	-6.395	-3.347	3.048	80.9
equatorial	5.887	-5.959	-3.374	2.585	92.9
trans-2	6.773	-6.259	-3.265	2.993	119.2
trans-1	7.197	-5.197	-3.537	1.660	158.1
$C_{20}Cl_2$					
cis-1	3.236	-6.068	-3.347	2.721	112.9
cis-2	4.725	-6.449	-3.456	2.993	76.4
equatorial	6.599	-5.987	-3.456	2.531	91.9
trans-2	7.620	-6.313	-3.374	2.939	113.9
trans-1	8.111	-5.279	-3.483	1.796	145.2
$C_{20}Br_2$					
cis-1	3.440	-5.987	-3.320	2.667	105.5
cis-2	4.912	-6.395	-3.456	2.939	71.4
equatorial	6.851	-5.932	-3.456	2.476	85.3
trans-2	7.856	-6.259	-3.347	2.912	107.6
trans-1	8.339	-5.225	-3.483	1.742	130.7
$C_{20}(OH)_2$					
cis-1	2.731	-5.714	-2.993	2.721	117.4
cis-2	4.119	-6.014	-2.966	3.048	95.8
equatorial	5.996	-5.578	-3.020	2.558	104.2
trans-2	6.829	-5.905	-2.884	3.020	133.1
trans-1	7.326	-4.844	-3.048	1.796	178.0

Table 1. Total energies (a. u.) and relative energies (in parentheses, in units of kJ/mol) of $C_{20}X_2$ (X = H, F, Cl, Br, and OH) regioisomers. The energies were obtained through B3LYP/6-31G(d, p) calculations[a]

Derivative X	H	F	Cl	Br	OH
Regioisomers					
cis-1 C_{2v}	-762.751865	-961.214271	-1681.934361	-5904.957574	-913.189430
	(0.0)	(0.0)	(0.0)	(0)	(0.0)
cis-2 C_s	-762.743522	-961.208593	-1681.929456	-5904.950848	-913.177126
	(21.9)	(14.9)	(12.9)	(17.7)	(32.3)
equatorial C_2	-762.740911	-961.205001	-1681.926233	-5904.947696	-913.174317
	(28.8)	(24.3)	(21.3)	(25.9)	(39.7)
trans-2 C_{2v}	-762.749522	-961.212952	-1681.933535	-5904.954771	-913.182852
	(6.2)	(3.5)	(2.2)	(7.4)	(17.3)
trans-1 D_{3d}	-762.717080	-961.162670	-1681.890710	-5904.914041	-913.137208
	(91.3)	(135.5)	(114.6)	(114.3)	(137.1)

[a]The relative energy is the difference between the energy of each regioisomer with different symmetry and the energy of the regioisomer (*cis*-1) with C_{2v} symmetry.

obtain geometries with a higher accuracy, we used the convergence criterion with tight optimization and an ultrafine grid of a pruned (99,590) grid (using the keywords Opt = Tight, Grid = ultrafine). We analyzed the relative energies and the HOMO and LUMO orbitals of the regioisomers.[20] Here we obtained the strain energy of the cage, which is the single point energy of naked C_{20} cage obtained from the optimized structure of each regioisomer minus the energy of optimized neutral C_{20} cage.

Results and Discussion

By performing calculations for the full optimization of the atomic structures of the $C_{20}X_2$ (X = H, F, Cl, Br, and OH) regioisomers at the level of B3LYP/6-31G(d, p) without any constraint, we obtained the relative energies of the regioisomers with C_{2v} (*cis*-1), C_s (*cis*-2), C_2 (*equatorial*), C_{2v} (*trans*-2), and D_{3d} (*trans*-1) symmetries, as shown in Table 1, under the reinforced tight convergence criterion. Here, the cutoffs on the forces and step size are reduced by the pruned (99,590) grid (keywords Opt = Tight, Grid = ultrafine) used to obtain accurate geometries. The atomic structures, HOMOs, and LUMOs of the regioisomers of each $C_{20}X_2$ derivative are shown in Figure 2. In addition, by analyzing the effect of the diadducts on the strain in the most stable cage of neutral C_{20} with D_{2h} symmetry, we obtained the strain energies of

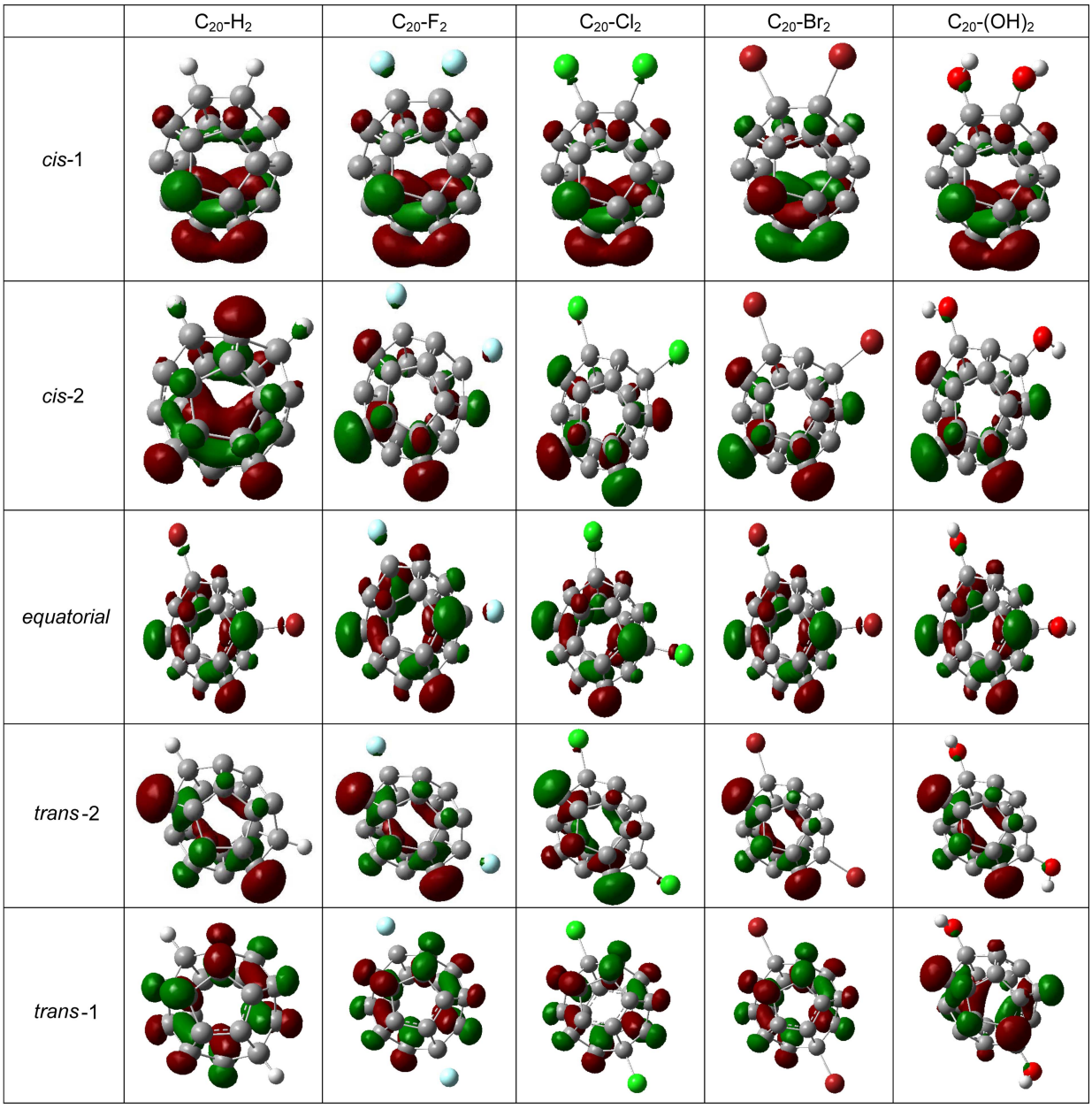

(a) The HOMOs of $C_{20}X_2$ regioisomers (isovalue = 0.05).

Figure 2. The HOMOs (a) and LUMOs (b) of fully optimized geometries of five $C_{20}X_2$ regioisomers at the level of B3LYP/6-31G(d, p). Here, X = H, F, Cl, Br, and OH.

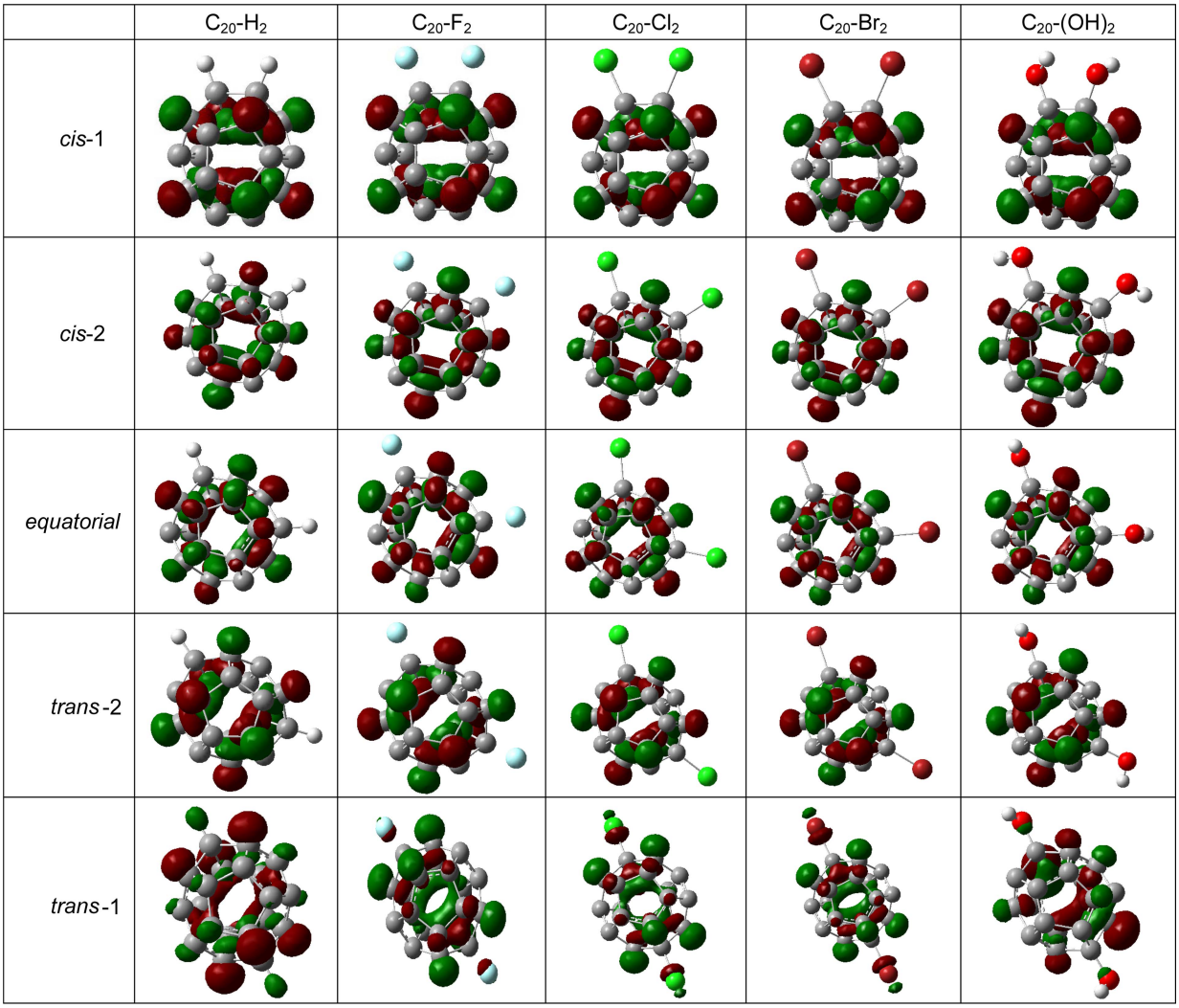

(b) The LUMOs of $C_{20}X_2$ regioisomers (isovalue = 0.05).

Figure 2. Continued

the regioisomers of each $C_{20}X_2$ derivative, as shown in Table 2.

Although the cage is formed exclusively from pentagons, the relative energies of the regioisomeric $C_{20}X_2$ derivatives with respect to symmetry has not been determined with certainty to date at the level of first principle calculations. Thus, in this study, we considered five regioisomers for each $C_{20}X_2$-derivative cage geometry obtained by full optimization and reinforced optimization. Among the five cage isomers whose geometries were fully optimized, the relative energies of the C_{2v} cage structures (*cis*-1, *trans*-2) with higher symmetry were lower than those of the C_s (*cis*-2) and C_2 (*equatorial*) isomers with lower symmetry and that of the D_{3d} isomer (*trans*-1) with the highest symmetry. The results showed that the energies of the regioisomers are in the following increasing order: *cis*-1 (C_{2v}) < *trans*-2 (C_{2v}) < *cis*-2 (C_s) < *equatorial* (C_2) < *trans*-1 (D_{3d}). The energies of the regioisomers were in the order *cis*-2 (C_s) < *equatorial* (C_2) < *trans*-1 (D_{3d}), which correlated with the increasing order in the strain energy for the neutral C_{20} cage isomer (D_{2h}: ground state). The calculated results showed that the addition of H, F, Cl, Br, and OH atoms releases the strain energy of C_{20} by pyramidalization of the two carbons of the cage. The hydrogenation, fluorination, chlorination, bromination, and hydroxylation reactions for all regioisomers of C_{20} were highly exothermic; in the case of the *trans*-2 regioisomer, for example, the values were –3.521, –7.357, –3.792, –3.029, and –7.662 eV, respectively. After the reaction takes place, electronic stability can be enhanced.

Thus, it is interesting to see that in the cage diadducts, the regioisomers with C_{2v} symmetry were more stable than the isomers with other symmetries, implying that the C_{20} cage for *cis*-1 with C_{2v} symmetry would exhibit the least strain deformation, compared to the parent cage with D_{2h} symmetry. However, our model calculations for the deformed cages of the C_{20} diadduct regioisomers suggested that the dispersion interaction if the distance between the two adducts of the cage derivatives is within the van der Waals

distance should be a stronger factor than is the deformation strain of the naked cage. Here, the distance between the two adducts was within the van der Waals distance only for the *cis*-1 regioisomer.[21] Thus, the most stable regioisomer was *cis*-1 with C_{2v} symmetry, followed by *cis*-2 (C_s), *equatorial* (C_2), and *trans*-1 (D_{3d}), but not *trans*-2 (C_{2v}). Therefore, it should be understood that while the strength of the cage distortion and the van der Waals force are important competing factors, the resonance effect caused by the delocalization of electrons also plays a crucial role in deciding the relative stability of the cage diadducts (see Tables 1 and 2).

Figure 2 shows the HOMOs and LUMOs for the regioisomers of the C_{20} diadducts. Table 2 presents the strain energies and the HOMO-LUMO gap energies of the regioisomers in Figure 2. Although the predominant electronic configurations of the regioisomers with the same symmetry for C_{20} diadducts are similar, the HOMOs and LUMOs of regioisomers with the different symmetry of geometrical structures are different in these regioisomers, implying that we can anticipate an entirely different set of characteristic chemical reactions for each HOMO and LUMO.

For the regioisomers, the effect of the adduct atom on the frontier orbitals of D_{2h} C_{20} is shown in Figure 2. The HOMO and LUMO energies of $C_{20}F_2$, $C_{20}Cl_2$, and $C_{20}Br_2$ are lower than those of C_{20} (HOMO: −5.034 eV; LUMO: −3.102 eV). In the case of all the $C_{20}H_2$ and $C_{20}(OH)_2$ regioisomers, the HOMO energies are lowered, but the LUMO energies are higher than that of C_{20}. As a result, C_{20} and $C_{20}X_2$ have different energy gaps, as shown in Table 2. The HOMO and LUMO energy gaps of all the *trans*-1 regioisomers are higher than those of C_{20} but are the lowest among those of the regioisomers with the same adducts; this trend is consistent with the fact that the strain energies of *trans*-1 regioisomers are very high. All the *trans*-2 regioisomers have the largest energy gaps, which shows that the two adducts can remarkably stabilize the C_{20} fullerene.

Conclusion

We obtained fully optimized geometries without any constraint at the B3LYP/6-31G(d) level by the hybrid density-functional method for regioisomers of the $C_{20}X_2$ cage (the smallest fullerene diadducts). The effect of two adducts on the atomic structures of the isomers showed that the relative energy of the C_{20} diadduct regioisomers is exceedingly dependent on the distance between the two adducts. Therefore, it is interesting to see that the isomeric species with the lowest energy is the medium-symmetry C_{2v}, and not D_{3d} (highest symmetry) or C_2 and C_s (reduced symmetry).

Although the predominant electronic configurations of the isomers are almost the same, the HOMO and LUMO maps are different among the five regioisomers of $C_{20}X_2$ (X = H, F, Cl, Br, and OH). Thus, an entirely different set of characteristic chemical reactions is expected for the HOMO and LUMO of each regioisomer, and this would be verified empirically.

Acknowledgments. This study was supported by Wonkwang University in 2009.

References

1. Kroto, H. W. *Nature* **1987**, *329*, 529.
2. Schmalz, T. Z.; Seitz, W. A.; Klein, D. J.; Hite, D. G. *J. Am. Chem. Soc.* **1998**, *110*, 1113.
3. Prinzbach, H.; Weiler, A.; Landenberer, P.; Wahl, F.; Wörth, J.; Scott, L. T.; Gelmont, M.; Olevano, D.; Issendorff, B. von. *Nature* **2000**, *407*, 60.
4. Hirsch, A. *The Chemistry of Fullerenes*; New York: Thieme, 1994.
5. Sabirov, D. S.; Bulgakov, R. G.; Khursan, S. L. *Arkivoc* **2011**, 8, 200-224.
6. Scheumann, K.; Sackers, E.; Bertau, M.; Leonhardt, J.; Hunkler, D.; Fritz, H.; Wörth, J.; Prinzbach, H. *J. Chem. Soc., Perkin Trans.* **1998**, *2*, 1195.
7. Prinzbach, H.; Wahl, F.; Weiler, A.; Landenberer, P.; Wörth, J.; Scott, L. T.; Gelmont, M.; Olevano, D.; Sommer, F.; Issendorff, B. von. *Chem. Eur. J.* **2006**, *12*, 6268.
8. Okamoto, Y. Chem. *Phys. Lett*. **2003**, *368*, 224.
9. Zhang, C.; Sun, W.; Cao, Z. *J. Chem. Phys.* **2007**, *126*, 144306.
10. Lee, J.; Lee, C.; Park, S. S.; Lee, K. H. Bull. *Korean Chem. Soc*. **2011**, *32*, 277-280.
11. Moran, D.; Simmonett, A. C.; Leach, F. E., III.; Allen, W. D.; Schleyer, P. v. R.; Schaefer, H. F., III. *J. Am. Chem. Soc.* **2006**, *128*, 9342.
12. An, Y.-P.; Yang, C.-L.; Wang, M.-S.; Ma, X.-G.; Wang, D.-H. *J. Phys. Chem. C* **2009**, *113*, 15756.
13. Irikura, K. K. *J. Phys. Chem. A* **2008**, *112*, 983.
14. Zhang, C.-Y.; Wu, H.-S.; Jiao, H. *J. Mol. Model* **2007**, *13*, 499.
15. (a) Beck, A. D. *J. Chem. Phys*. **1993**, *98*, 5648. (b) Lee, C.; Yang, W.; Parr, R. G. *Phys. Rev. A* **1988**, *37*, 785.
16. Stephen, P. J.; Devlin, F. J.; Chablowski, C. F.; Frisch, M. J. *J. Phys. Chem.* **1994**, *98*, 11623.
17. Herteing, R. H.; Koch, W. *Chem. Phys. Lett.* **1997**, *268*, 345.
18. Hehre, W. J.; Ditchfield, R.; Pople, J. A. *J. Chem. Phys.* **1972**, *56*, 2257.
19. Frisch, M. J. *et al.* A Gaussian 03 B.04, Gaussian, Inc., Pittsburgh, PA, 2003.
20. Clark, T. R.; Koch, R. *The Chemist's Electronic Book of Orbitals*; Springer-Verlag: Berlin, 1999.
21. Bond, A. *J. Phys. Chem.* **1964**, *68*, 441.